Available online at www.sciencedirect.com
ScienceDirect
Polymer 48 (2007) 458–466
polymer
www.elsevier.com/locate/polymer

Morphology control of various aromatic polyimides by using phase separation during polymerization

Kanji Wakabayashi, Shin-ichiro Kohama, Shinichi Yamazaki, Kunio Kimura*

Graduate School of Environmental Science, Okayama University, 3-1-1 Tsushima-naka, Okayama 700-8530, Japan

Received 2 September 2006; received in revised form 30 November 2006; accepted 30 November 2006
Available online 19 December 2006

Abstract

Morphology control of various aromatic polyimides representative as poly(4,4′-oxydiphenylene pyromelliteimide) was examined by using the phase separation during solution polymerization. Polymerizations of aromatic dianhydrides and aromatic diamines to the polyimides were carried out in poor solvents at 240–330 °C for 6 h with no stirring. Polymerization concentrations were from 0.25% to 3.0%. The polyimides were obtained as yellow precipitates. Two categorized morphologies were created, which were particles and crystals exhibiting lath-like and plate-like habits. These morphologies of polyimides could be selectively controlled by the polymerization conditions. The higher concentrations, less miscible solvents and lower temperatures were preferable to yield the particles via liquid–liquid phase separation. On the contrary, the lower concentration, miscible solvents and higher temperature were desirable to yield the crystals. The polyimide precipitates showed high crystallinity and possessed excellent thermal stability at which the 10 wt% loss temperatures in N_2 were in the range of 590–694 °C.

Keywords: Polyimide; Morphology; Phase separation

1. Introduction

Aromatic polyimides are characterized by their outstanding thermal and mechanical properties and they have been attracted as high performance polymer materials [1–3]. Their properties strongly depend on not only their chemical structure but also their morphology including molecular orientation. However, it is too difficult to afford the desirable morphology to obtain the essential properties predicted from the chemical structure because of their intractability. In order to overcome this problem, several approaches have been conducted for the morphology control of polyimides; one is an improvement of their processability by chemical modifications such as copolymerization or introduction of bulky pendant group into the main chain [4–6], and another is a preparation by the two-step synthesis including the synthesis of the soluble poly(amic acid) precursor and the following imidization. The preparation of oriented polyimide films and fibers from poly(amic acid) precursors has been numerously studied so far [6–8]. However, the former approach reduces the molecular rigidity and the potential performance of original polyimides is sacrificed to get processability. Even in the later, the catenation of *para* and *meta* linkages of poly(amic acid) precursors and the rapid crystallization during imidization prevent from the orientation of polymer molecules. Additionally, the elimination of by-products during cyclization generates the defects like pinholes in the polyimide products [9].

We have been studying the morphology control of rigid aromatic polymers during solution polymerization [10–15]. Lozenge-shaped crystals and microspheres of poly(*p*-phenylene pyromelliteimide) were prepared as precipitates by the polymerization of pyromellitic dianhydride (PMDA) and 1,4-phenylene diamine (PPDA) [16]. These products were formed by reaction-induced phase separation. They possessed extremely high crystallinity and outstanding thermal stability. We herein apply this morphology control method using the

* Corresponding author. Tel./fax: +81 86 251 8902.
E-mail address: polykim@cc.okayama-u.ac.jp (K. Kimura).

0032-3861/$ - see front matter © 2006 Elsevier Ltd. All rights reserved.
doi:10.1016/j.polymer.2006.11.061

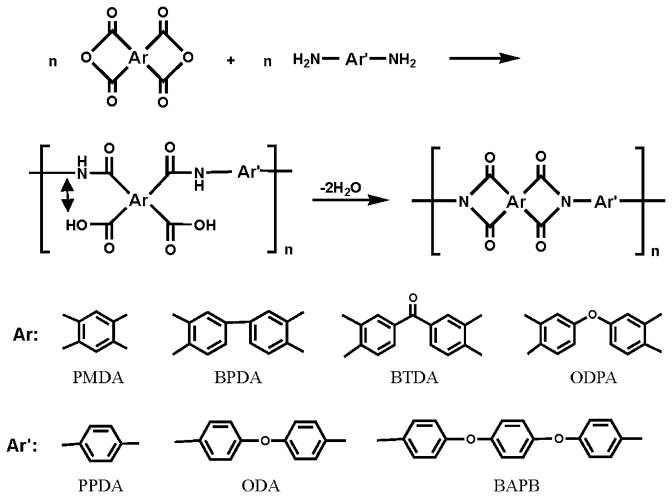

Scheme 1. Synthesis of various polyimides.

reaction-induced phase separation of oligomers to various aromatic polyimides depicted in Scheme 1 in order to create new morphologies.

2. Experimental section

2.1. Materials

PMDA was purchased from Aldrich Co. Ltd. and used after sublimation. 3,3′,4,4′-Biphenyltetracarboxylic dianhydride (BPDA), 3,3′,4,4′-benzophenonetetracarboxylic dianhydride (BTDA), 4,4′-oxydiphthalic anhydride (ODPA), 4,4′-oxydianiline (ODA) and 1,4-bis(aminophenoxy)benzene (BAPB) were purchased from Tokyo Kasei Co. Ltd. and used as received. PPDA was a gift of Taishin Kasei Kogyo Co. Ltd. and also used as received. Liquid paraffin (LPF) was purchased from Nacalai Tesque Co. Ltd. and purified by distillation (185–215 °C/0.2 mmHg). Therm S-1000 (a mixture of isomers of dibenzyltoluene) (TS10) was purchased from Nippon Steel Chemical Co. Ltd. and also purified by distillation (165–175 °C/0.2 mmHg). Diphenyl sulfone (DPS) was purchased from Tokyo Kasei Co. Ltd. and purified by recrystallization from a mixture of methanol and water.

2.2. Measurements

Morphology of the products was observed on a HITACHI S-3500N scanning electron microscope. Samples were dried, sputtered with platinum/palladium and observed at 20 kV. Average shape parameters of the products were determined by taking the average of over 200 observation values. Infrared (IR) spectra were recorded on a JASCO FT/IR-410 spectrometer. The inherent viscosity (η_{inh}) of polyimides was measured in concentrated sulfuric acid at 0.5 g dL^{-1} and 30 °C. WAXS powder patterns were recorded on a RIGAKU MiniFlex diffractometer at 30 kV and 15 mA with a scanning rate of 1° min^{-1}. Thermogravimetric analysis (TGA) was performed on a Perkin–Elmer TGA-7 with a scanning rate of 20 °C min^{-1} in N_2. The degree of imidization (DI) was calculated from the intensity ratio of the imide band at 1380 cm^{-1} (C–N stretching) to the reference band at 1500 cm^{-1} (C=C stretching of 1,4-phenylene group) in the IR spectra, according to the reported procedure [17]. Matrix-assisted laser desorption ionization time-of-flight mass spectrometry (MALDI-TOF MS) was performed on a Bruker Daltonics Auto FLEX MALDI-TOF MS system operating with a 337-nm N_2 laser. Spectra were obtained in the linear positive mode with an accelerating potential of 20 kV. Mass calibration was performed with angiotensin I (MW 1296.69) and insulin B (MW 3496.96) from a Sequazyme peptide mass standard kit. The samples were then prepared by the evaporation–grinding method and ran in 3-aminoquinoline as a matrix doped with potassium trifluoroacetate salt according to the reported procedure [18].

2.3. General procedure for the synthesis of polyimides

PMDA (0.057 g, 0.26 mmol) and 20 mL of TS10 were placed into a cylindrical flask equipped with a gas inlet tube, and the reaction mixture was heated with stirring in N_2. PMDA was entirely dissolved at ca. 240 °C. When the solution was heated at 280 °C, ODA (0.052 g, 0.26 mmol) was added into the solution under stirring. The stirring was stopped in 5 s and then the polymerization was carried out at 280 °C for 6 h with no stirring. The solution became immediately turbid due to the precipitation of oligomers. After 6 h, the yellow precipitates were filtrated at 280 °C, and then washed with *n*-hexane and acetone, and then dried at 100 °C for 12 h. The filtrate was poured into *n*-hexane and the precipitates were collected, which were dissolved at 280 °C in the solution.

3. Results and discussion

3.1. Morphology control of PI(PMDA/ODA)

Polyimides prepared from various aromatic dianhydrides and aromatic diamines are abbreviated as the combination of the name of dianhydrides and diamines in this study. For example the polyimides prepared from PMDA and ODA were described as PI(PMDA/ODA), which are commercially named Kapton. The morphology control of PI(PMDA/ODA) was first examined. Polymerizations were carried out in three different solvents such as LPF, TS10 and DPS at a concentration of 0.25–3.0% for 6 h. Polymerization temperature was changed from 240 to 330 °C. PMDA and ODA were not dissolved in these solvents at room temperature. PMDA was first dissolved in the solvent by heating and then solid ODA was added into the solution at the polymerization temperature. After the addition of ODA, the solution became turbid immediately and then the polymers were formed as yellow precipitates. Polymerization results are summarized in Table 1. IR spectrum of the products prepared in run no. 1 is shown in Fig. 1 as a representative.

The characteristic bands of the imide group such as C=O stretching, C–N stretching and C–N bending appeared clearly at 1720, 1380 and 720 cm^{-1}, respectively, and those of amic

Table 1
Polymerization results of PI(PMDA/ODA)

Run no.	Polymerization conditions			Yield (%)	Morphology[a]	η_{inh}[b] (dL g^{-1})	Average diameter of particles and SP products[c] (μm)	10 wt% loss temp[d] (°C)
	Concentration (%)	Solvent	Temp (°C)					
1	3.0	TS10	280	99.9	Particle	1.08	0.56 (51.0%)	648
2	1.0	TS10	280	92.0	Lath, SP	0.95	1.24 (27.1%)	650
3	0.5	TS10	280	73.0	Lath, SP	1.17	1.32 (18.0%)	645
4	0.25	TS10	280	32.0	Plate, lath, SP	0.89	1.99 (23.1%)	634
5	1.0	LPF	280	98.7	Particle	0.93	0.63 (34.5%)	659
6	1.0	DPS	280	58.5	Plate	0.40	–	603
7	0.5	TS10	240	81.3	SP, particle	0.82	0.79 (28.5%)	651
8	0.5	TS10	330	65.2	SP	1.38	2.09 (14.0%)	652

[a] SP stands for the spherical product comprised with plate-like crystals.
[b] Measured in concentrated sulfuric acid at 0.5 g dL^{-1} and 30 °C.
[c] Numbers in parentheses are the coefficient of variation (%) of diameter.
[d] Measured on TGA at the rate of 20 °C min^{-1} in nitrogen.

acid moieties were not detected at all. The resulting polymers have high viscosities of 0.40–1.17 dL g^{-1} comparable to those prepared by the low temperature polymerization [19], despite being prepared through the precipitation of oligomers. This fact indicates that PI(PMDA/ODA) was prepared as precipitates through the formation of amic acid and the following imidization.

Morphologies of the precipitates were roughly categorized by two types, of which one was plate-like and/or lath-like and another was spherical, as shown in Fig. 2. The average diameter of the spherical products was in the range of 0.56–0.79 μm with the coefficient of variation (cv) from 28.5% to 51.0%. The surfaces of these nanoparticles were slightly rough. The lath-like crystals were 2–10 μm in length, 0.4–2.5 μm in width and approximately 0.1 μm in thickness. The surface was very hilly and there were many splinters along the long axis of the crystal. Small size plate-like crystals were aggregated to form the spherical products (SP) of which the diameter of the aggregates was 1.24–2.09 μm and its cv value was 14.0–27.1%. The morphology of the SP was obviously different from the former particles.

These morphological features are highly related to the polymerization conditions. Polymerization concentration influences the morphology significantly (run nos. 1–4). When the polymerization was carried out at a concentration higher than 1.0%, the particles were formed. On the contrary, the mixtures of lath-like crystals and SP were obtained at a concentration less than 1.0%. These morphologies are generated by the phase separation of oligomers, and therefore the difference in the morphology is brought about by the difference in the phase separation behaviors of the oligomers. Reaction-induced phase separation of oligomers in poor solvent is describable on the analogous concentration–temperature phase diagram (C–T phase diagram) to that of the partially miscible polymer–solvent system [20,21]. The phase separation curve in the repulsive system can be written as the combination of the freezing point curve of the oligomers and the upper critical solution temperature type consolution curve. The oligomers are formed by the polymerization reaction, and the molecular weight of oligomers increases in the solution. When the molecular weight of oligomers exceeds a critical value, the oligomers are in the supersaturated state and then phase-separated. If the supersaturated oligomers are across the freezing point curve, they are precipitated by the crystallization to form the crystals, and the polymer crystals are finally formed by the post-polymerization in the crystals [10]. On the other hand, if they are across the consolution curve, the oligomers are precipitated through liquid–liquid phase separation and the microdroplets of the dense phase are generated in the dilute phase. Finally, polymer particles are formed due to the solidification of the fine droplets caused by the further polymerization in them [15]. On the basis of this C–T phase diagram, the influence of the polymer concentration on the morphology is explainable as follows: at a concentration less than 1.0%, the higher molecular weight oligomers are phase-separated through supersaturated state, bringing about the shift of the freezing point curve toward the higher temperature. Therefore the oligomers crystallize to form the crystals. On the other hand, the lower molecular weight oligomers are formed at the higher concentration and then precipitated via liquid–liquid phase separation to form the fine droplets due to the decrease in the freezing point. The particles are ultimately obtained. The yield of the precipitates became higher with the increase in the concentration. The polymerization proceeds faster and the lower molecular weight oligomers are precipitated at higher concentration as discussed, leading to the higher yield. To confirm this discussion, the oligomers left in the solution

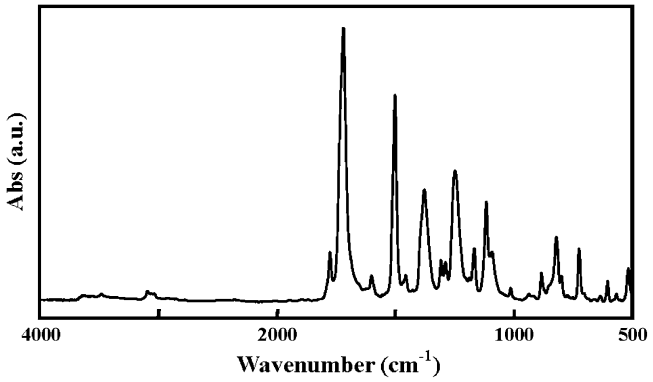

Fig. 1. IR spectrum of PI(PMDA/ODA) prepared in run no. 1.

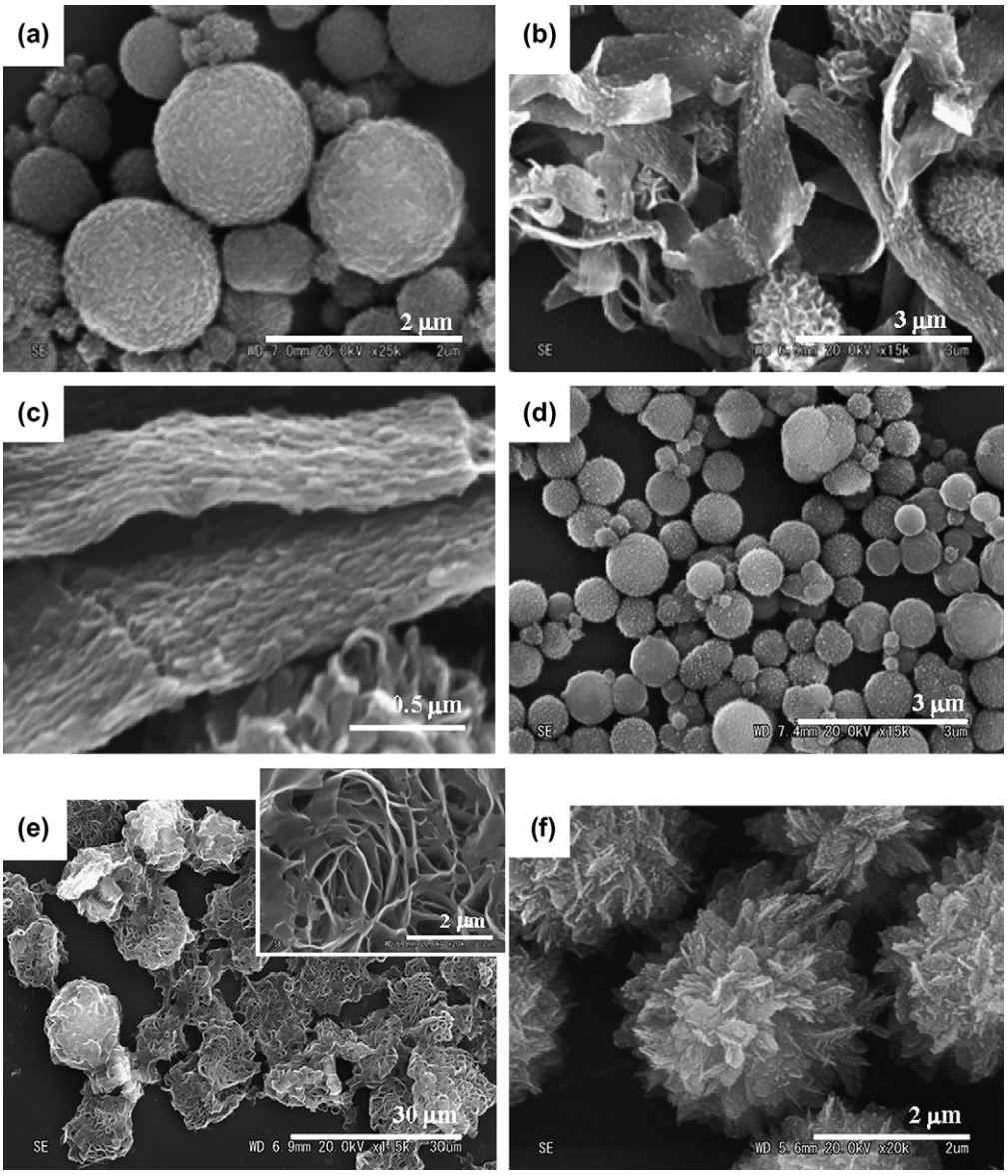

Fig. 2. Morphologies of PI(PMDA/ODA) prepared in (a) run no. 1, (b) and (c) run no. 3, (d) run no. 5, (e) run no. 6 and (f) run no. 8.

after 6 h were collected and analyzed by the MALDI-TOF mass spectroscopy. The spectra are shown in Fig. 3 (run nos. 3 and 4) and the peaks were assigned according to the previous paper [18]. The dissolved oligomers were the mixtures of the quite low molecular weight adducts including imide and amic acid moieties. The higher molecular weight oligomers were detected in run no. 4 than in run no. 3. This fact reveals that the lower molecular weight oligomers were precipitated at a higher concentration and this supports the above discussions.

Characteristics of the solvent also influenced the morphology as well as the concentration (run nos. 2, 5 and 6). LPF is inclined to form the particles, and TS10 and DSP are inclined to form the crystals. The yields of the product prepared at a concentration of 1.0% at 280 °C in LPF, TS10 and DPS were 98.7%, 92.0% and 58.5%, respectively. This result suggests that the miscibility between the oligomers and the solvents might increase in the order of LPF, TS10 and DPS. Here, the solubility parameters (δ) of these solvents and PI(PMDA/ODA) are compared to evaluate the miscibility. The δ of LPF and PI(PMDA/ODA) are 8.3 [22] and 10.7 $(\mathrm{cal\,cm^{-3}})^{1/2}$ [23]. The δ of TS10 and DPS were estimated according to the Fedors' group contribution method [24] and they are 10.6 and 11.2 $(\mathrm{cal\,cm^{-3}})^{1/2}$, respectively. These results reveal that the miscibility increases in the order of LPF < DPS ≅ TS10. This is roughly in agreement with the order estimated from the yields. These morphological features can also be explained in $C-T$ phase diagram. The lower molecular weight oligomers are phase-separated in LPF due to the lower miscibility. The freezing point curve shifts toward the lower temperature and the consolution curve shifts toward the higher temperature. The shifts of these curves make two immiscible liquid phases' region wider and the liquid–liquid phase separation is induced to form the particles. In contrast to this, the higher molecular weight oligomers are precipitated

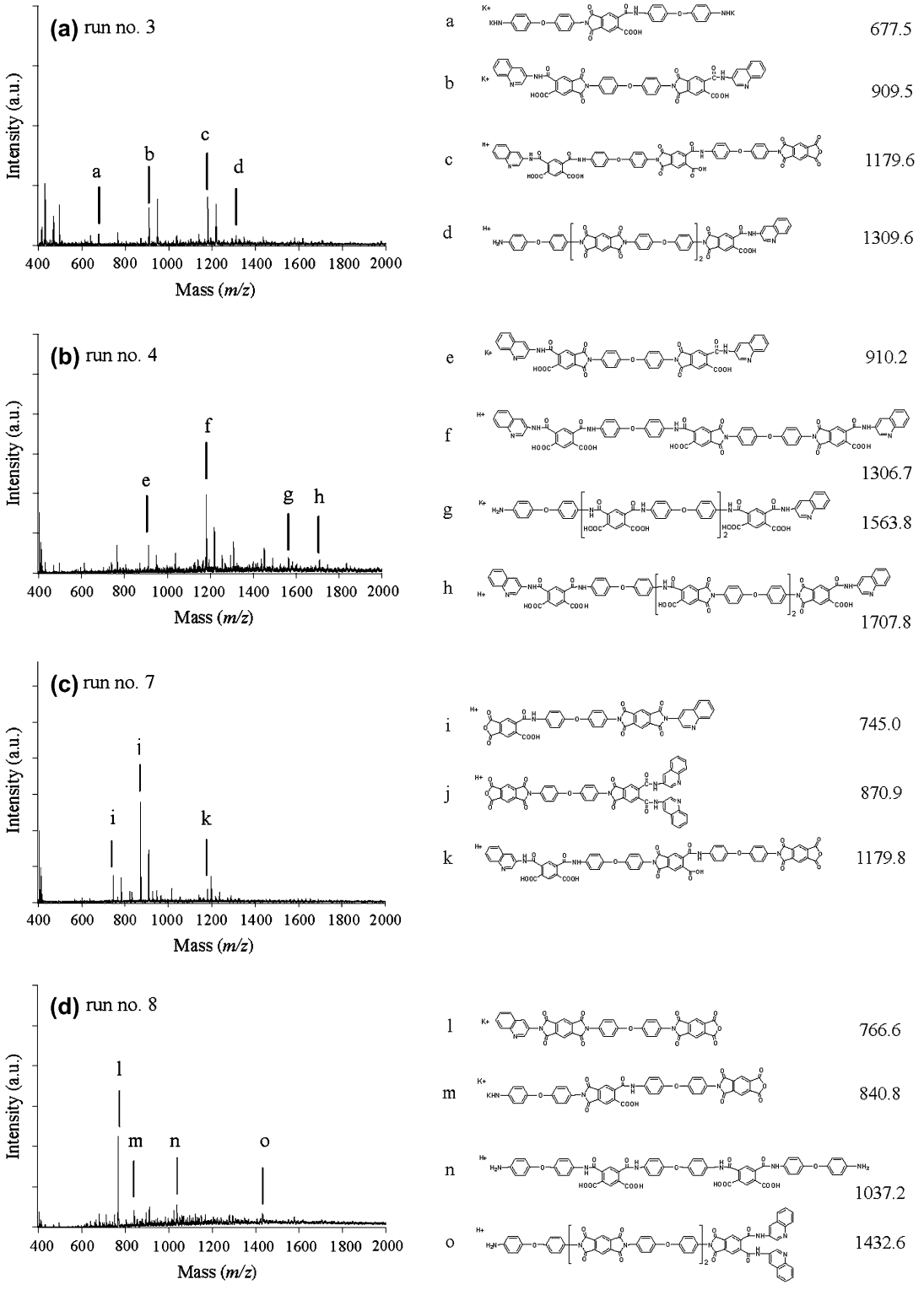

Fig. 3. MALDI-TOF mass spectra of oligomers collected from solution prepared at the condition of (a) run no. 3, (b) run no. 4, (c) run no. 7 and (d) run no. 8.

via crystallization in TS10 and DPS to form the crystals due to the higher miscibility.

Polymerization temperature also influences the morphology (run nos. 3, 7 and 8). The crystals were formed at a temperature higher than 280 °C, and the particles were formed at the lower temperature. The influence of the polymerization temperature on the morphology seems likely not to be identical with that of other aromatic polymers [15]. Liquid–liquid phase separation is readily induced at higher temperature as explained in the $C-T$ phase diagram. The precipitates collected right after the phase separation were analyzed in order to estimate the chemical structure of the phase-separated oligomers. Fig. 4

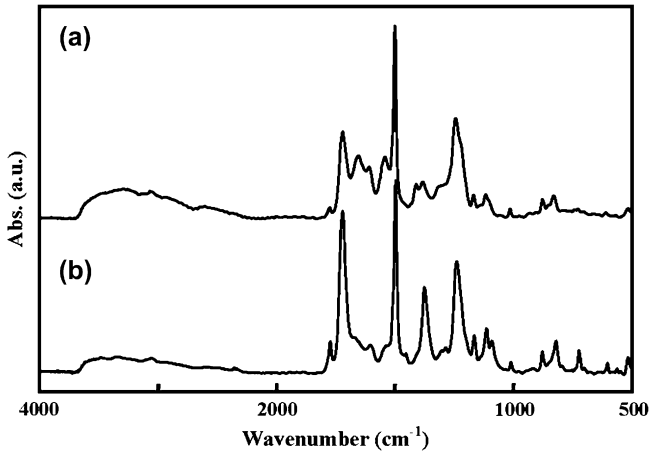

Fig. 4. IR spectra of precipitates collected just after phase separation at addition temperature of (a) 240 and (b) 280 °C.

shows the IR spectra of the precipitates prepared at 240 and 280 °C. The characteristic bands of the imide group described in Fig. 1 were clearly observed in spectrum of the precipitates prepared at 280 °C. Although these bands were also detected in the spectrum of the products at 240 °C, their relative intensities were quite low. Further the bands of amide C═O stretching and carboxylic acid C═O stretching were observed at 1665 and 1715 cm^{-1}, respectively. The broad bands of amide N–H stretching and carboxylic acid O–H stretching were also observed at 3500–3000 cm^{-1}. This result suggests that the amic acid moiety in the oligomer was transformed to the imide group by thermal imidization with the elimination of water and the chemical structures of the phase-separated oligomers are different between 240 and 280 °C. The DI of the precipitates and the oligomer collected from the solution was calculated by using the intensity ratio of the imide C–N stretching relative to the aromatic C═C stretching according to the previous study [17]. They are plotted in Fig. 5 as a function of polymerization time.

With respect to the precipitates, the DI at 280 °C was 78.4% after 10 s and then increased to 100% after 2 min. On the other hand, the DI at 240 °C was 33.7% after 10 s and then increased to 89.0% after 2 min. With respect to the oligomers recovered from the solution, the DI at 240 °C increased slightly with time from 28.8% to 40.9% and that at 280 °C also increased with time from 34.8% to 57.6%. This difference in the DI at the initial stage of the polymerization indicates that the oligomers rich in imide moieties are formed at 280 °C in the solution and subsequently phase-separated. In contrast to this, the oligomers rich in amic acid moieties are phase-separated at 240 °C. Both the consolution curve and the freezing point curve of oligomers tend to shift toward higher temperature with increasing the content of imide groups due to the entropic contribution caused by the increase in the rigidity. These shifts bring about the expansion of the crystallization region in the $C-T$ phase diagram, and hence the oligomers are precipitated to form the crystals at 280 °C. The oligomers containing much amic acid moieties have the lower freezing point curve due to the isomeric mixture of *para* and

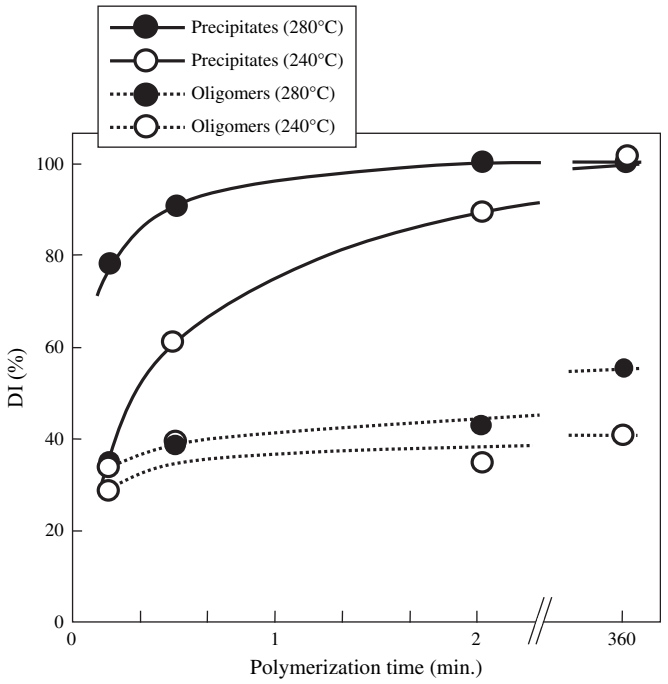

Fig. 5. Plots of DI of precipitates and oligomers dissolved in the solution at 240 and 280 °C.

meta catenations in amic acid moiety, resulting in the expansion of two immiscible liquid phases. Therefore, the oligomers prepared at 240 °C tend to be precipitated via the liquid–liquid phase separation, leading to the formation of the particles. Additionally, both the structural irregularity caused by the catenations and the formation of the intermolecular hydrogen bonding through amic acid moiety lower the crystallizability of the oligomers, preventing the formation of the crystals. Thus, the morphologies of polyimides are quite susceptible to the DI of the oligomers phase-separated from solution. The yields of the precipitates prepared at a concentration of 0.5% at 240, 280 and 330 °C in TS10 were 81.3%, 73.0% and 65.2%, respectively. They increased with the decrease in the temperature. This fact suggests that the lower temperature makes the critical molecular weight for the precipitation lower due to the decrease in the miscibility as aforesaid, leading to the increase in the yield. The oligomers left in the solution after 6 h were collected and analyzed by the MALDI-TOF mass spectroscopy as also shown in Fig. 3 (run nos. 3, 7 and 8). The molecular weight of the oligomers left in the solution at 240 °C was clearly lower than others and this result is identical with the above discussions.

WAXS intensity profiles of the products prepared at various temperatures in TS10 are shown in Fig. 6. Broad halo attributed to amorphous parts was observed in the profile of the particles prepared at 240 °C and the particles showed low crystallinity. On the contrary, the reflection peaks in the profiles of the crystals prepared at 280 and 330 °C were clearly sharp and the amorphous halos were significantly diminished. These crystals possessed high crystallinity. The observed peaks can be assigned by the reported orthogonal unit cell

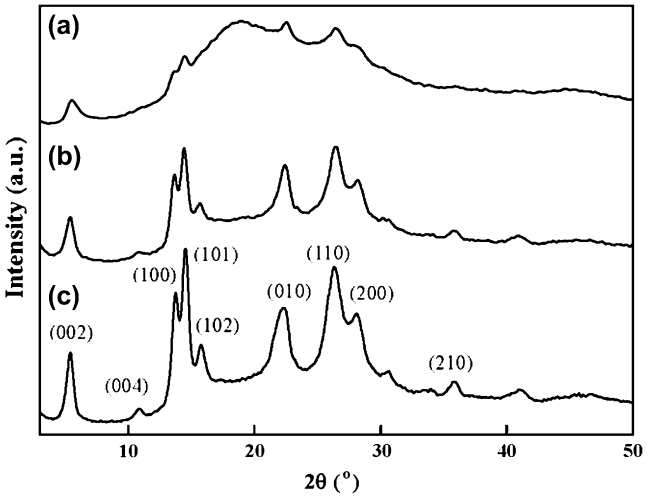

Fig. 6. WAXS intensity profiles of PI(PMDA/ODA). (a) Microspheres prepared at 240 °C, (b) crystals prepared at 280 °C and (c) crystals prepared at 330 °C.

of PI(PMDA/ODA) as shown in Fig. 6 [25]. With respect to the thermal stability, the 10 wt% loss temperature of PI(PMDA/ODA) was reported as around 530 °C in N_2 prepared by the usual two-step synthesis via soluble poly(amic acid) precursors [26,27]. The temperatures of 10 wt% loss of the precipitates in this study were in the range of 603–659 °C and they were 100 °C higher as shown in Table 1.

3.2. Morphology control of other polyimides

The morphology control method using phase separation was next applied to other six polyimides. Polymerization conditions and results are summarized in Table 2. In these polymerizations, the products were also obtained as precipitates. The chemical structures of these precipitates were analyzed by IR spectroscopy. The characteristic bands of imide group were clearly observed in their spectra as shown in Fig. 7. Further, the bands of amic acid moiety were not detected. These

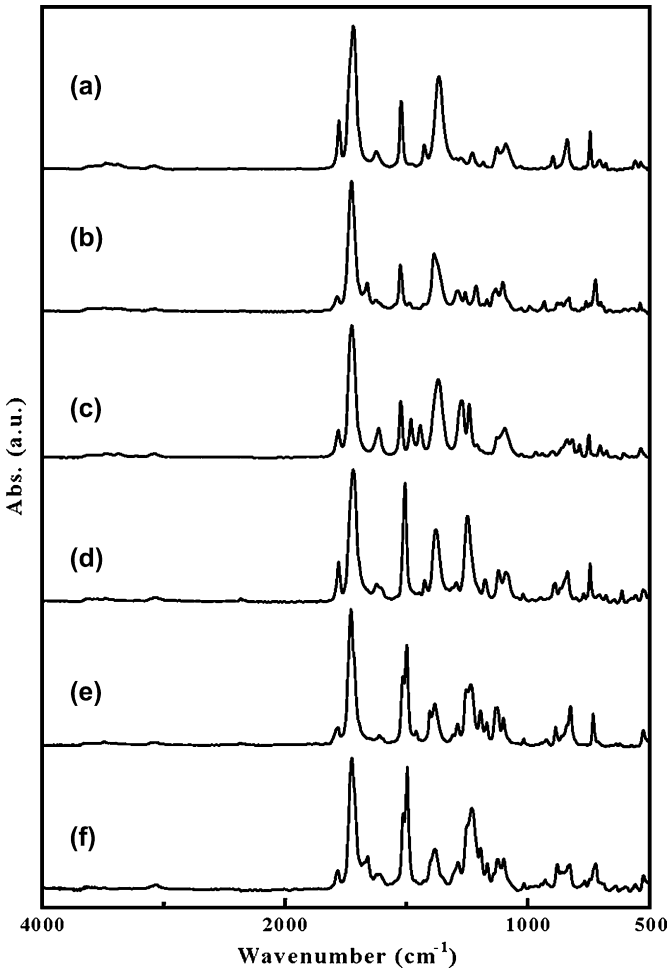

Fig. 7. IR spectra of various polyimides prepared through phase separation of oligomers. (a) PI(BPDA/PPDA) (run no. 9), (b) PI(BTDA/PPDA) (run no. 11), (c) PI(OPDA/PPDA) (run no. 13), (d) PI(BPDA/ODA) (run no. 16), (e) PI(PMDA/BAPB) (run no. 17) and (f) PI(BTDA/BAPB) (run no. 19).

polyimides might possess higher miscibility to the solvents than PI(PMDA/ODA) and due to this the yields of the precipitates were slightly lower than that of PI(PMDA/ODA). The

Table 2
Polymerization results of various polyimides

Run no.	Polymer code	Polymerization conditions				Morphology[a]	η_{inh}[b] (dL g^{-1})	10 wt% loss temp[c] (°C)
		Concentration (%)	Solvent	Temp (°C)	Yield (%)			
9	PI(BPDA/PPDA)	1.0	TS10	280	82.0	SP, particle	0.63	694
10		1.0	DPS	280	97.9	Plate	0.78	663
11	PI(BTDA/PPDA)	0.5	TS10	280	89.5	SP, particle	1.03	670
12		0.5	DPS	280	62.0	Plate	0.32	589
13	PI(ODPA/PPDA)	0.5	TS10	240	68.6	Particle	0.29	596
14		0.5	TS10	280	42.1	SP	0.75	633
15	PI(BPDA/ODA)	1.0	LPF	280	95.4	Particle	0.98	628
16		1.0	TS10	280	59.1	Plate	1.40	631
17	PI(PMDA/BAPB)	0.5	TS10	280	61.6	SP	—[d]	611
18		0.5	TS10	240	78.0	SP, particle	—[d]	622
19	PI(BTDA/BAPB)	0.5	TS10	280	50.8	SP	0.97	590
20		0.5	TS10	240	64.3	Particle	1.02	599

[a] SP stands for the spheres comprised with plate-like crystals.
[b] Measured in concentrated sulfuric acid at 0.5 g dL^{-1} and 30 °C.
[c] Measured on TGA at a heating rate of 20 °C min^{-1} in nitrogen.
[d] Insoluble in sulfuric acid.

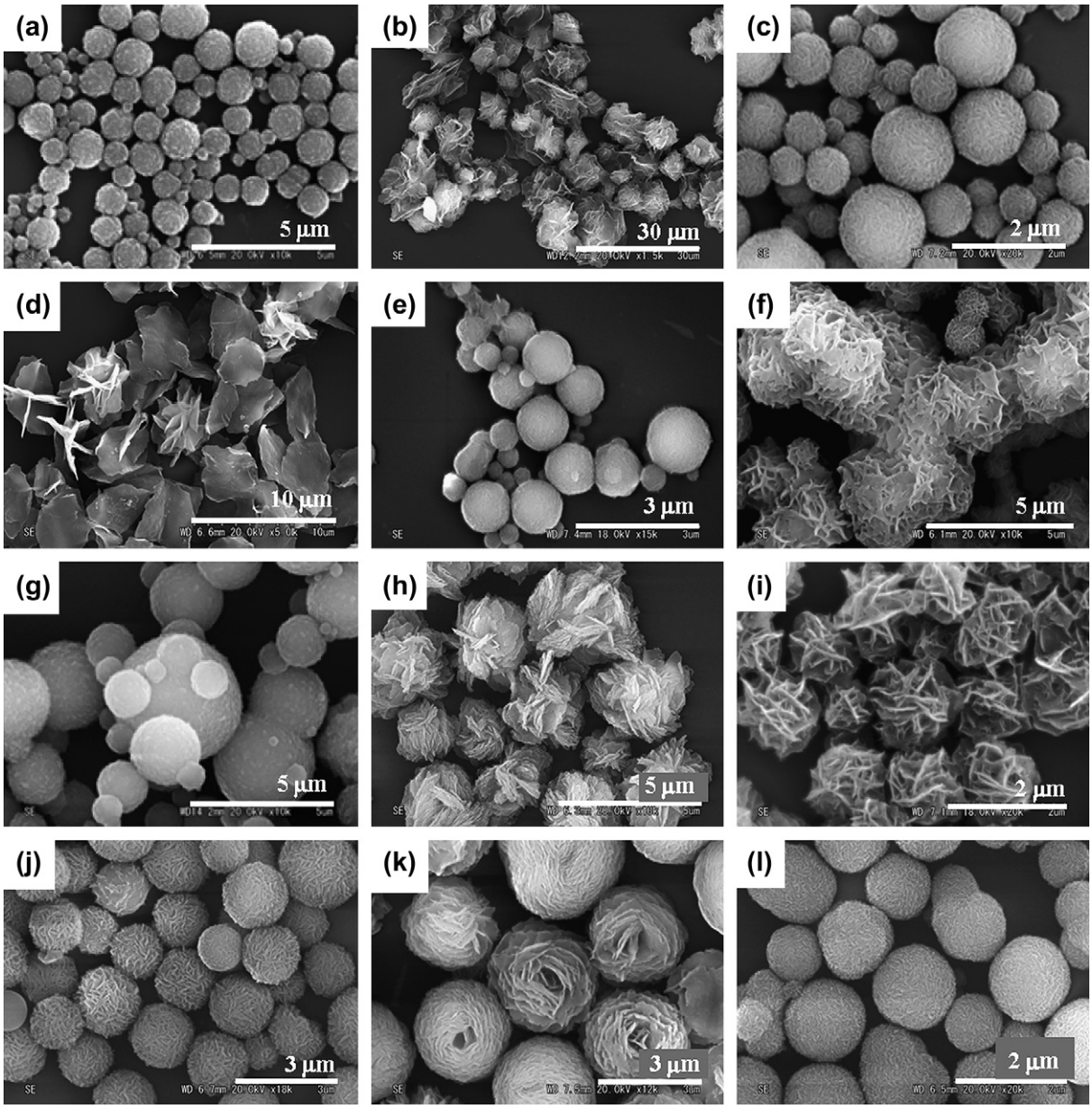

Fig. 8. Morphologies of various polyimides prepared through phase separation of oligomers. (a) PI(BPDA/PPDA) (run no. 9), (b) PI(BPDA/PPDA) (run no. 10), (c) PI(BTDA/PPDA) (run no. 11), (d) PI(BTDA/PPDA) (run no. 12), (e) PI(ODPA/PPDA) (run no. 13), (f) PI(ODPA/PPDA) (run no. 14), (g) PI(BPDA/ODA) (run no. 15), (h) PI(BPDA/ODA) (run no. 16), (i) PI(PMDA/BAPB) (run no. 17), (j) PI(PMDA/BAPB) (run no. 18), (k) PI(BTDA/BAPB) (run no. 19), and (l) PI(BTDA/BAPB) (run no. 20).

precipitates except PI(PMDA/BAPB) had high inherent viscosities of 0.29–1.40 dL g^{-1}. PI(PMDA/BAPB) was insoluble in concentrated sulfuric acid. All these precipitates prepared for 6 h were identified as fully cyclized polyimides having high molecular weight.

The morphologies of the products are also categorized by two types as well as PI(PMDA/ODA), which are particles and plate-like crystals. The typical morphologies are shown in Fig. 8. These morphological features strongly suggest that the particles and the crystals are formed via the liquid–liquid phase separation and the crystallization of oligomers, respectively. The influences of the polymerization conditions such as temperature, concentration and the character of the solvent on the morphology were basically similar to those for PI(PMDA/ODA) as already discussed.

WAXS intensity profiles of the obtained crystals are shown in Fig. 9. They exhibit crystalline nature. Among them, the plate-like crystals of PI(BTDA/PPDA), PI(PMDA/BAPB) and PI(BTDA/BAPB) show extremely high crystallinity. These polyimides prepared by the two-step synthesis via soluble poly(amic acid) precursors are usually known as amorphous and not crystallizable polymers. However, since they were prepared by the crystallization of oligomers in this study, they exhibit high crystallinity. This preparation procedure affords crystalline polyimides. The 10 wt% loss temperatures in N_2 were in the range of 590–694 °C measured on TGA and

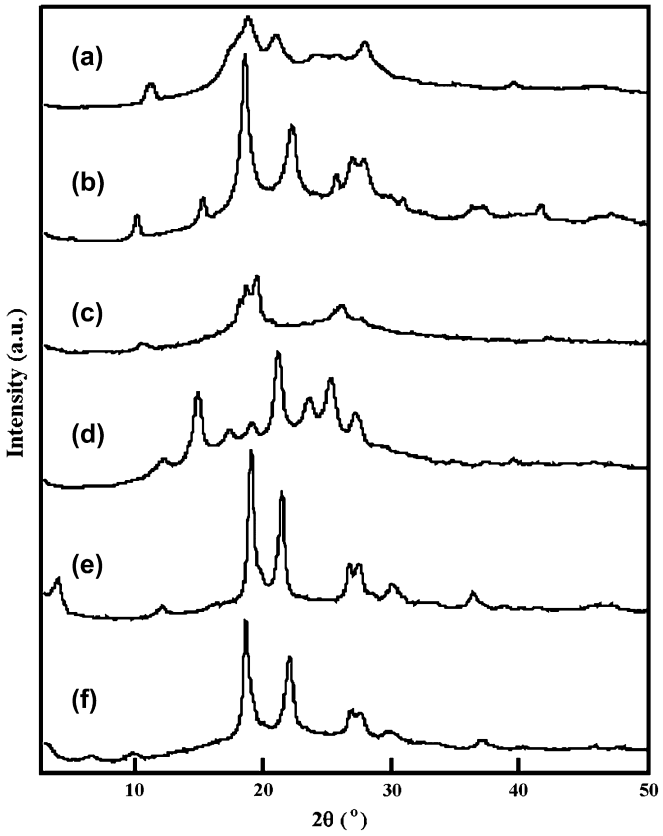

Fig. 9. WAXS intensity profiles of various polyimides prepared through phase separation of oligomers. (a) PI(BPDA/PPDA) (run no. 9), (b) PI(BTDA/PPDA) (run no. 12), (c) PI(ODPA/PPDA) (run no. 14), (d) PI(BPDA/ODA) (run no. 16), (e) PI(PMDA/BAPB) (run no. 17) and (f) PI(BTDA/BAPB) (run no. 19).

they show outstanding thermal stability. Especially, PI(BPDA/PPDA) exhibits the highest thermal stability and it is in the highest class of thermal stability in the organic polymers.

4. Conclusions

Two categorized morphologies were created by using the phase separation during the solution polymerization. The one was spherical and the other was crystalline such as lath-like and plate-like habits. These morphologies of polyimides could be selectively verified by the polymerization conditions such as concentration, solvent and temperature. The higher concentrations, less miscible solvents and lower temperatures were preferable to yield the particles via liquid–liquid phase separation. On the contrary, the lower concentration, miscible solvents and higher temperature were desirable to yield the crystals. With respect to the temperature, it influenced the DI of the phase-separated oligomers and the oligomers rich in imide groups were phase-separated at higher temperature via crystallization. At lower temperature, the phase-separated oligomers were rich in amic acid moieties leading to the liquid–liquid phase separation to form the particles ultimately. The polyimide precipitates showed high crystallinity and possessed excellent thermal stability.

Acknowledgement

This study was supported by Industrial Technology Research Grant Program from New Energy and Industrial Technology Development Organization (NEDO) of Japan.

References

[1] Sroog CE. J Polym Sci Macromol Rev 1976;11:161.
[2] Bessonov MI, Koton MM, Kudryavtsev VV, Laius LA. Polyimides: thermally stable polymers. New York: Consultants Bureau; 1987.
[3] Wilson D, Stenzenberger HD, Hergenrother PM. Polyimides. New York: Blackie; 1990.
[4] Jinta T, Matsuda T. Sen'i Gakkaishi 1986;42:554.
[5] For example Cassidy PE. Thermally stable polymers, syntheses and properties. New York: Marcel Dekker; 1980.
[6] Mittal KL. Polyimides, synthesis, characterization, and application, vol. 1. New York: Plenum Press; 1984.
[7] Dine-hart RA, Wright WW. J Appl Polym Sci 1967;11:609.
[8] Salem JR, Sequeda FO, Duran J, Lee WY, Yang RM. J Vac Sci Technol 1989;A4:369.
[9] Mittal KL. Polyimides, synthesis, characterization, and application, vol. 2. New York: Plenum Press; 1984.
[10] Yamashita Y, Kimura K. Polymeric materials encyclopedia. Boca Raton, FL: CRC Press; 1996. p. 8707.
[11] Yamashita Y, Kato Y, Endo S, Kimura K. Makromol Chem Rapid Commun 1988;9:687.
[12] Kimura K, Endo S, Kato Y, Yamashita Y. Polymer 1994;35:123.
[13] Kimura K, Endo S, Kato Y, Yamashita Y. Polymer 1993;34:1054.
[14] Kimura K, Kato Y, Inaba T, Yamashita Y. Macromolecules 1995;28:255.
[15] Kimura K, Inoue H, Kohama S, Yamashita Y, Sakaguchi Y. Macromolecules 2003;36:7721.
[16] Kimura K, Zhuang J-H, Wakabayashi K, Yamashita Y. Macromolecules 2003;36:6292.
[17] Lee HJ, Won J, Park HC, Lee H, Kang YS. J Membr Sci 2000;178:35.
[18] Gies AP, Nonidez WK, Anthamatten M, Cook RC, Mays JW. Rapid Commun Mass Spectrom 2002;16:1903.
[19] Wallach ML. J Polym Sci Part A-2 1969;7:1995.
[20] Richards RB. Trans Faraday Soc 1946;42:10.
[21] Flory PJ, Mandelkern L, Hall HK. J Am Chem Soc 1951;73:2532.
[22] Tate S, Watanabe Y, Chiba A. Polymer 1993;34:4974.
[23] Hoontrakul P, Pearson RA. Prepr ACS Polym Mater Sci Eng 2002;87:387.
[24] Fedors RF. Polym Eng Sci 1974;14:147.
[25] Kazarayan LG, Tsvankin DY, Ginzburg BM, Tuichiev S, Korzhabin LN, Frenkel SN. Vysokomol Soedin 1972;A14:1199.
[26] Korshak VV. Heat-resistant polymers. Jerusalem: Israel Program for Scientific Translations; 1971.
[27] Bessonov MI, Kuznetsov NP, Koton MM. Vysokomol Soedin 1978;20A(2):347.